Supporting Information

Constructing a built-in electric field by anchoring highly dispersed Zn single atoms on UiO-66-NH_2 for efficient CO_2 photoreduction

Mingna Chu [a], Yang Li [a, *], Ximing Chen [a], Guangyao Hou [b], Yan Zhou [a], Hongjun Kang [a, b],Wei Qin [b], Xiaohong Wu[a, *]

[a] MIIT Key Laboratory of Critical Materials Technology for New Energy Conversion and Storage, School of Chemistry and Chemical Engineering, Harbin Institute of Technology, Harbin 150001, P. R. China.

[b] School of Materials Science and Engineering, Harbin Institute of Technology, Harbin, Heilongjiang 150001, PR China

*Corresponding author, E-mail address: liyang198517@hit.edu.cn (Y. Li); wuxiaohong@hit.edu.cn (X. Wu).

Table of Contents

1. Characterization

Characterization techniques: X-ray diffraction (XRD) was used Cu Kα radiation and the range of 2θ is from 5° to 60°to characterize the crystal structure (D/max-2500, Rigaku, Japan). The morphology of the samples was analyzed by transmission electron microscopy (TEM) on Jem-2100F Jeol apparatus with an acceleration voltage of 200 kV. The FEI Tecnai G2 F20 equipped with Energy-dispersive X-ray (EDX) detector was employed to access element analyses of the samples. The Fourier-transform infrared (FT-IR) spectra with KBr as diluents were carried out using Avatar 360 (Nicolet Instrument Corporation, US). Electronic states were analyzed by X-ray photoelectron spectroscopy (XPS) on an ESCALAB 250 Xi apparatus. The UV–vis diffuse reflectance spectra (DRS) were gained on a UV–vis spectrophotometer (UV-vis DRS, Shimadzu UV-2450) with $BaSO_4$ as the white standard.

2. Other measurements

2.1. XAFS Measurements and Analysis.

The X-ray absorption spectra (XAS) of the samples at Zn K-edge，including X-ray absorption near-edge structure (XANES) and extended X-ray absorption fine structure (EXAFS), was collected at the Singapore Synchrotron Light Source (SSLS) center, in which a pair of channel-cut Si (111) crystals was used in the monochromator. The Zn K-edge XANES data were recorded in transmission mode. Zn foil and ZnO were used as references. The operating energy of storage ring was 2.5 GeV and the average electron current was less than 200 mA. The obtained EXAFS data were extracted and processed using the ATHENA module of the IFEFFIT software packages according to standard procedures.

2.2. Photoelectrochemical measurements

The photoelectrochemical measurements were conducted in a traditional three-electrode syste m with 0.2 M Na_2SO_4 solution as the electrolyte. The prepared photocatalyst, a platinum plate and a saturated KCl Ag/AgCl electrode were used as working electrode, counter electrode and reference electrode,

respectively, which were collected on an electrochemical station (CHI760E, China) under 300W xenon lamp. All experiments were conducted at room temperature (about 25 °C). Mott−Schottky plots of photocatalysts were obtained with the same three-electrode system in N_2-purged 0.5M Na_2SO_4 electrolyte solution.

2.3. The apparent quantum yield (AQY)

The apparent quantum yield (AQY) measurement for photocatalytic CO_2 reduction was carried out employing a 300 W Xenon lamp fitted with a different band-pass filter. When a 365 nm band-pass filter was used, the irradiation area and the light intensity were 5 cm^2 and 21.12 mW cm^{-2}, respectively. The mass of photocatalysts was 50 mg. The AQY was calculated according to the following equation:

AQY = Ne/Np*100% = $\left(2M_{CO} + 8M_{CH_4}\right)$ NAhc/SPtλ*100% (M_{CO}: the CO amount, M_{CH_4}: the CH_4 amount, NA: Avogadro constant, h: Planck constant, c: light speed, S: irradiation area, P: light intensity, t: reaction time, λ: the wavelength of light).

3. Density functional theory (DFT) calculation.

Density functional theory (DFT) calculation. DFT calculations were conducted through the Vienna ab-initio Simulation Package (VASP) with the projector augment wave method. Generalized gradient approximation of the Perdew-Burke-Ernzerhof (PBE) functional was used as the exchange-correlation functional. The calculations were based on the unit cell with the cutoff energy set to 450 eV and structural relaxation performed until the energy and force convergence criteria reached 1×10^{-4} eV and 0.02 eV $Å^{-1}$, respectively. The Gibbs free energy was calculated as $\Delta G = \Delta E + \Delta EZPE - T\Delta S$, where the ΔE, ΔEZPE, and ΔS are electronic energy, zero-point energy, and entropy difference between products and reactants. The zero-point energies of isolated and absorbed intermediate products were calculated from the frequency analysis.

4. Supporting Figures

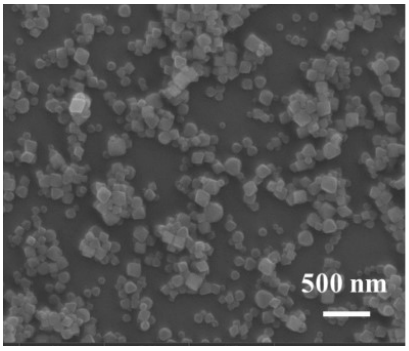

Fig. S1. SEM images of UiO-66-NH_2.

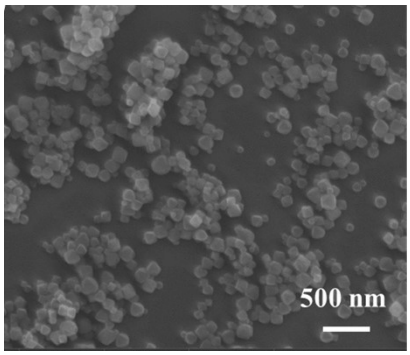

Fig. S2. SEM images of UiO-66-NH_2-0.7Zn SAs.

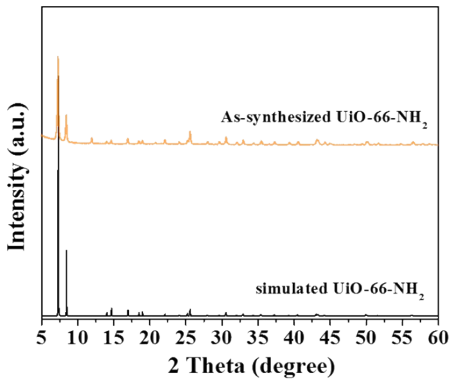

Fig. S3. XRD patterns of simulated UiO-66-NH_2 and as-synthesized UiO-66-NH_2.

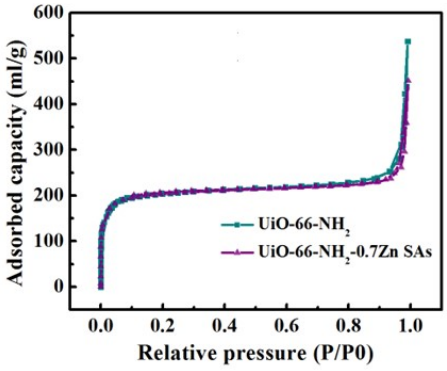

Fig. S4. N_2 adsorption-desorption isotherms of UiO-66-NH_2 and (b) UiO-66-NH_2-0.7Zn SAs.

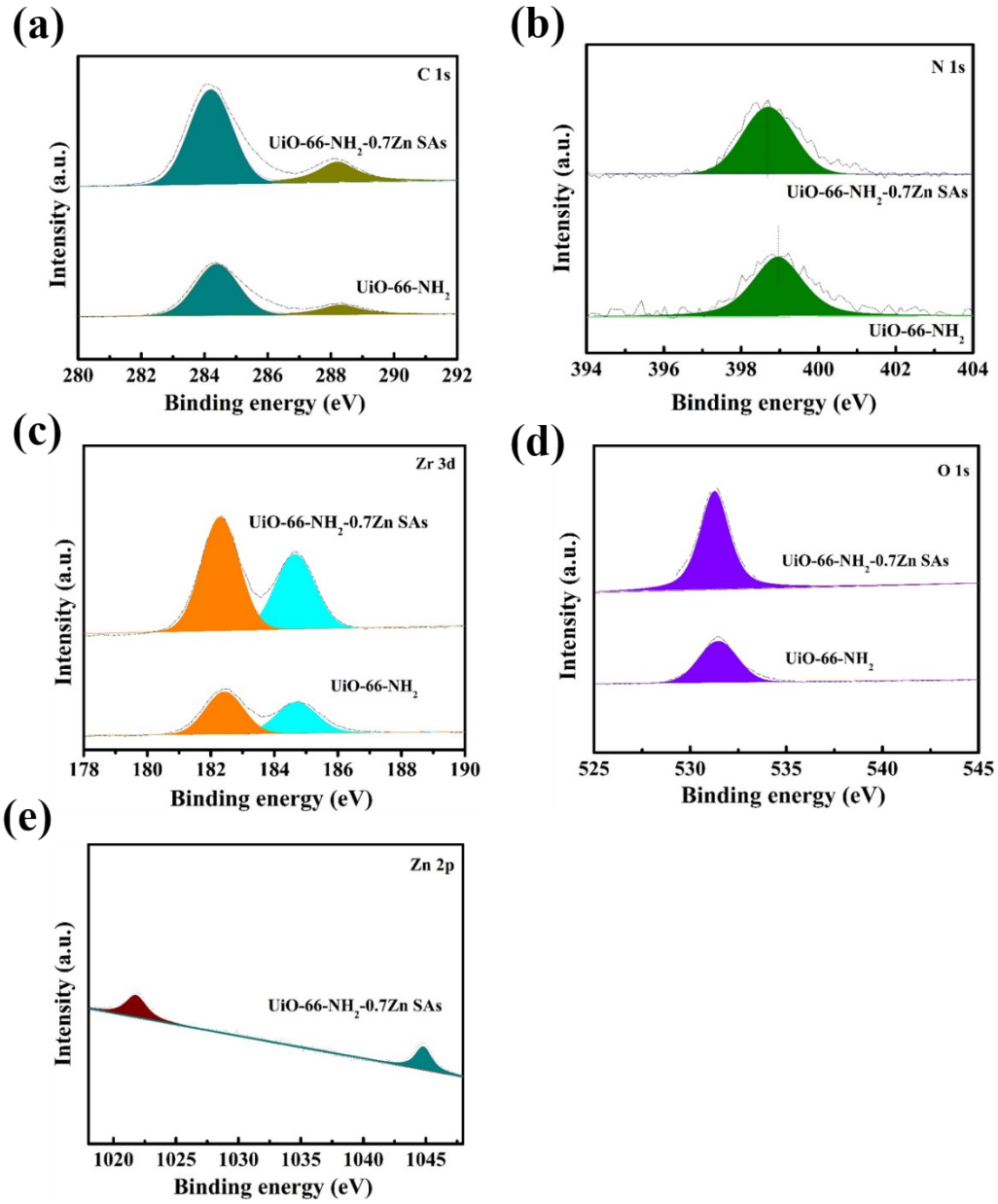

Fig. S5. XPS spectra of (a) C 1s, (b) N 1s, (c) Zr 3d, (d) O 1s and (e) Zn 2p of different samples.

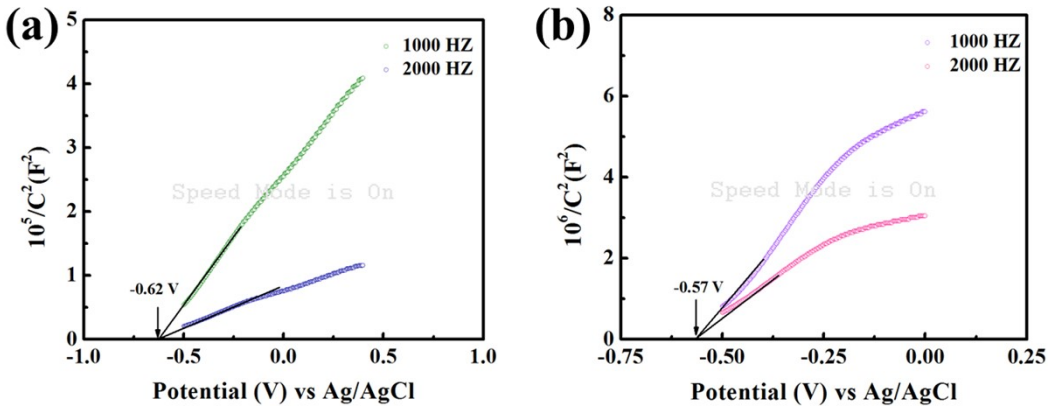

Fig. S6. Mott-Schottky plots for (a) UiO-66-NH_2 and (b) UiO-66-NH_2-0.7Zn SAs.

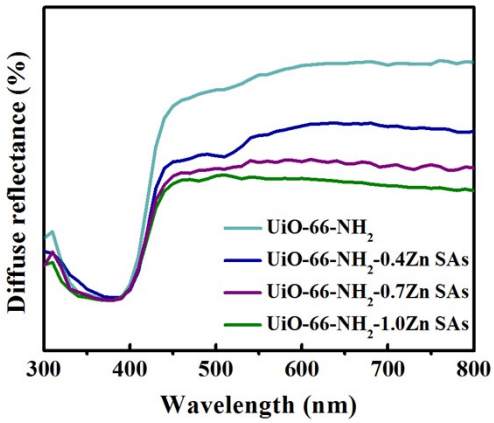

85

86 **Fig. S7.** DRS spectra of different samples.

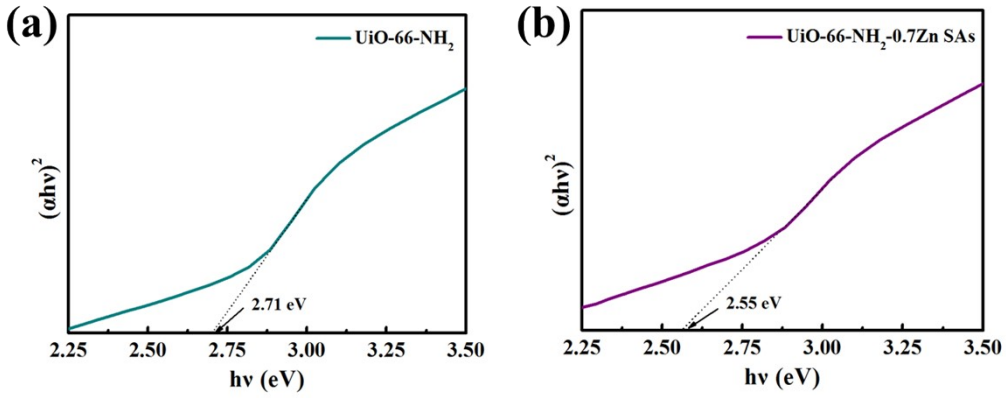

87

88 **Fig. S8.** The plots of $(\alpha h\nu)^2$ vs $(h\nu)$ for (a) UiO-66-NH_2 and (b) UiO-66-NH_2-0.7Zn SAs.

89 The optical band gap energy (Eg) of a semiconductor material could be evaluated by thefollowing formula:

90 $$\alpha h\nu = A(h\nu - Eg)^{n/2}$$

91 where α, h, ν, A, and Eg represent the absorption coefficient, planck constant, light frequency, proportionality and band

92 gap energy, respectively. As shown in the Fig. S11, the Eg values for UiO-66-NH_2 and UiO-66-NH_2-0.7Zn SAs are

93 calculated to be 2.71 and 2.55 eV, respectively.

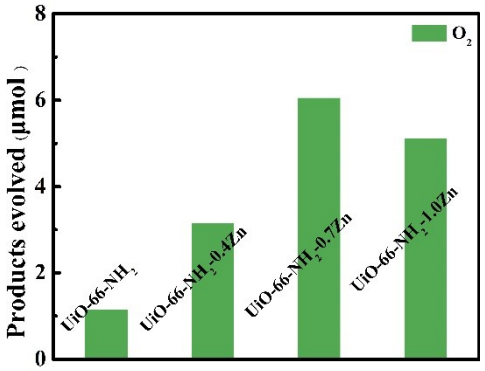

94

95 **Fig. S9.** Oxygen yield for 4 hours in photocatalytic CO_2 reduction process for different samples.

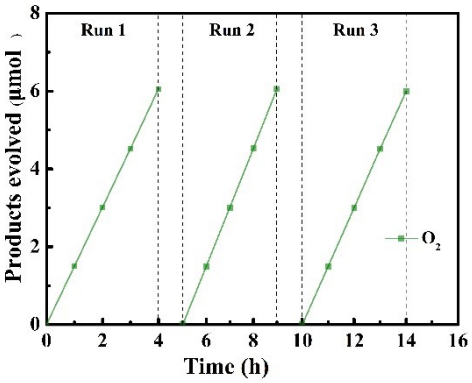

Fig. S10. Photocatalytic cycling test of UiO-66-NH_2-0.7Zn SAs.

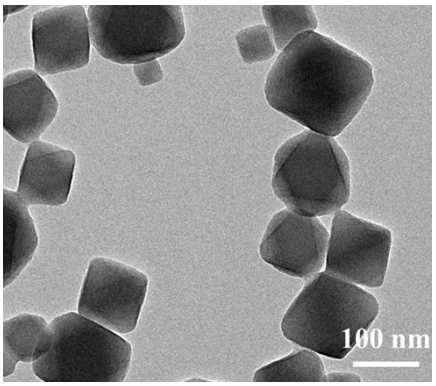

Fig. S11. TEM images of UiO-66-NH_2-0.7Zn SAs after after the cyclic tests

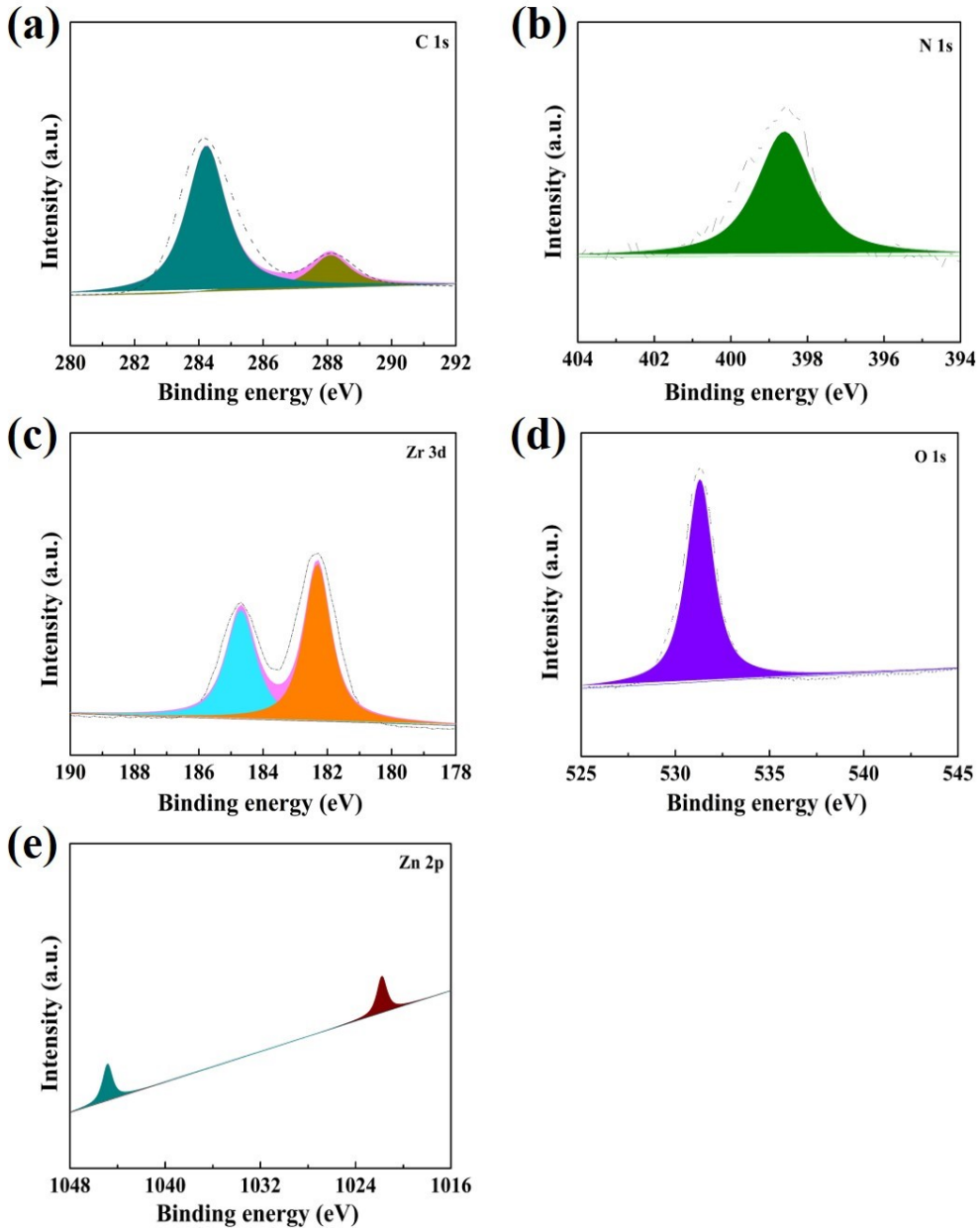

100

101 **Fig. S12.** XPS spectra of UiO-66-NH_2-0.7Zn SAs after the cyclic tests.

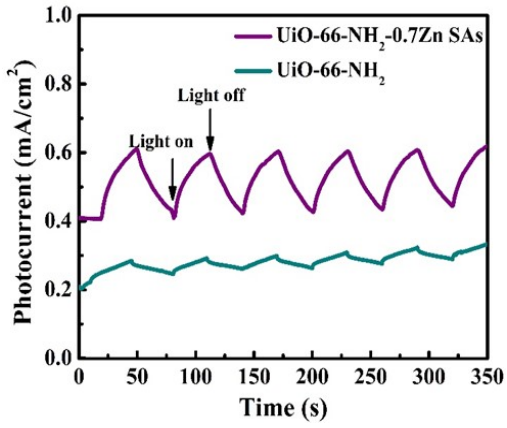

102

103 **Fig. S13.** Photoelectrochemical properties of UiO-66-NH_2 and UiO-66-NH_2-0.7Zn SAs.

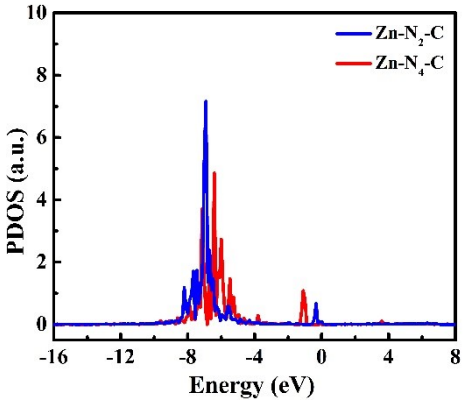

104

105 **Fig. S14.** PDOS plots of 3d of Zn for Zn-N mode.

106 ## 5. Supporting Tables

107 **Table S1.** S_{BET}, pore volume and pore diameter of UiO-66-NH_2 and UiO-66-NH_2-0.7Zn SAs

Samples	S_{BET}(m^2/g)	Pore volume(cm^3/g)	Pore diameter (nm)
UiO-66-NH_2	807.5935	0.8096	4.0099
UiO-66-NH_2-0.7Zn SAs	780.3318	0.6233	3.1951

108 **Table S2.** EXAFS fitting parameters at the Zn K-edge（S_0^2=0.91）

Sample	Path	C.N.	R (Å)	$\sigma^2\times10^3$ (Å^2)	ΔE (eV)	R factor
Zn	Zn-N	2.2±0.2	2.04±0.01	11.0±1.2	2.8±1.0	0.003

109 *C.N.*: coordination numbers; *R*: bond distance; σ^2: Debye-Waller factors; Δ*E*: the inner potential correction. *R* factor:

110 goodness of fit. * Fitting with fixed parameter.

111 **Table S3.** Comparison of photocatalytic CO_2 reduction performance of the reported photocatalysts.

Sample	CO evolution (μmol g^{-1} h^{-1})	Light source（W）	Ref.
TiO2@50 Cu	23.25	300W Xe lamp	Chem. Eng. J.[1]
0.7NiSA-5OB-CN	22.1	300W Xe lamp	Adv. Mater.[2]
$Bi_2Sn_2O_7$ NPs	14.88	300W Xe lamp	Appl. Catal. B: Environ.[3]
5T/15CN/BVNS	14.5	300W Xe lamp	Angew. Chem. Int. Ed.[4]
Ni-SA-x/ZrO_2	11.8	300W Xe lamp	Adv. Energy Mater.[5]
UiO-66-NH_2-0.7Zn SAs	40.23	300W Xe lamp	This work

112 **Table S4.** The AQY of 365 nm for photocatalytic CO_2 reduction over UiO-66-NH_2-0.7Zn SAs and UiO-66-NH_2.

Sample	Irradiation time (h)	The number of incident photons	CO evolution (μmol)	CH_4 evolution (μmol)	AQY (%)
UiO-66-NH_2-0.7Zn SAs	3	2.049×10^{21}	1.33	0.14	0.63
UiO-66-NH_2	3	2.049×10^{21}	7.43	0.88	0.11

The detailed calculation

$$Np = \frac{SPt\lambda}{hc} = \frac{5\ cm^2 \times 21.12 \times 10^{-3} J\ s^{-1}\ cm^{-2} \times 3 \times 3600s\ \times 365 \times 10^{-9} m}{6.626 \times 10^{-34} J\ s\ \times 3 \times 10^8\ m\ s^{-1}} = 2.094 \times 10^{21}$$

AQYUiO - 66 - NH_2

$$= \frac{N_e}{N_p} \times 100\% = \frac{\left(2M_{CO} + 8M_{CH_4}\right) \times N_A}{N_p} = \frac{(2 \times 1.33 + 8 \times 0.14) \times 10^{-6} \times 6.02 \times 10^{23}}{2.094 \times 10^{21}}$$
$$= 0.11\%$$

AQY$UiO - 66 - NH_2 - 0.7Zn\ SAs$

$$= \frac{N_e}{N_p} \times 100\% = \frac{(2M_{CO} + 8M_{CH_4}) \times N_A}{N_p} = \frac{(2 \times 7.43 + 8 \times 0.88) \times 10^{-6} \times 6.02 \times 10^{23}}{2.094 \times 10^{21}}$$
$$= 0.63\%$$

References

1 M. Liu, L. Zheng, X. Bao, Z. Wang, P. Wang, Y. Liu, H. Cheng, Y. Dai, B. Huang, Z. Zheng, Substrate-dependent ALD of Cux on TiO_2 and its performance in photocatalytic CO_2 reduction, Chem Eng J, 405 (2021) 126654.

2 Y. Wang, Y. Qu, B. Qu, L. Bai, Y. Liu, Z.-D. Yang, W. Zhang, L. Jing, H. Fu, Construction of Six-Oxygen-Coordinated Single Ni Sites on g-C_3N_4 with Boron-Oxo Species for Photocatalytic Water-Activation-Induced CO_2 Reduction, Advanced Materials, 33 (2021) 2105482.

3 S. Guo, J. Di, C. Chen, C. Zhu, M. Duan, C. Lian, M. Ji, W. Zhou, M. Xu, P. Song, R. Long, X. Cao, K. Gu, J. Xia, H. Liu, Y. Zhao, L. Song, Y. Xiong, S. Li, Z. Liu, Oxygen vacancy mediated bismuth stannate ultra-small nanoparticle towards photocatalytic CO_2-to-CO conversion, Applied Catalysis B: Environmental, 276 (2020) 119156.

4 J. Bian, Z. Zhang, J. Feng, M. Thangamuthu, F. Yang, L. Sun, Z. Li, Y. Qu, D. Tang, Z. Lin, F. Bai, J. Tang, L. Jing, Energy Platform for Directed Charge Transfer in the Cascade Z-Scheme Heterojunction: CO_2 Photoreduction without a Cocatalyst, Angewandte Chemie International Edition, 60 (2021) 20906-20914.

5 X. Xiong, C. Mao, Z. Yang, Q. Zhang, G.I.N. Waterhouse, L. Gu, T. Zhang, Photocatalytic CO_2 Reduction to CO over Ni Single Atoms Supported on Defect-Rich Zirconia, Advanced Energy Materials, 10 (2020) 2002928.